

Resistive film frequency selective rasorbers: from design, integration to function

Jiahua Yang , Kun Zhang , and Lan Yao ^{*} 

College of Textiles, Donghua University, No. 2999 North Renmin Road, Shanghai 201620, PR China

Received: 8 November 2025 / Accepted: 25 November 2025

Abstract. Resistive film frequency selective rasorbers (FSRs), as advanced electromagnetic metamaterials, seamlessly integrate the functions of out-of-band absorption and in-band transmission, enabling selective spatial control of electromagnetic waves. This review systematically summarizes recent research progress in this field. It begins by elucidating the fundamental operational principles. Then this review adopts a material-centric classification framework, providing a comprehensive and critical analysis of two major categories of resistive film FSRs: carbon-based film FSRs and indium tin oxide (ITO) film FSRs. As in some literature, the materials for the resistive films were not elucidated but the sheet resistance was given, a third category with the name of specified sheet resistance film FSRs was reviewed. And the fourth was dynamically tunable resistive film FSRs which could be achieved through the integration of resistive films and functional materials. For each category, it delves into the intrinsic material properties, design methodologies, achieved performance and application suitability. Finally, the article outlines prevailing challenges including multi-performance coordination and fabrication process limitations, and suggests promising future directions, such as film compositing, intelligent design, and system integration, thereby providing crucial insights for the development of novel integrated stealth and communication technologies.

Keywords: Resistive film / frequency selective rasorber / integration of absorption and transmission / metamaterials

1 Introduction

With the rapid advancement of modern electronic information technology, electromagnetic waves have become an indispensable medium in fields such as communications, radar, and wireless sensing. However, the accompanying electromagnetic interference (EMI) issues and increasingly severe electromagnetic detection threats pose significant challenges to the reliability of electronic systems and the survivability of military equipment [1–3]. Consequently, how to manage and control electromagnetic waves efficiently has become frontier research and a core demand in materials science and electronic engineering.

Conventional electromagnetic functional materials are typically designed for a single performance characteristic. For instance, wave-absorbing materials function by dissipating incident electromagnetic energy through dielectric loss (electric/magnetic loss) or ohmic loss,

whereby the electromagnetic energy is converted into thermal energy or other forms. Although designed to maximize electromagnetic energy dissipation, these materials often suffer from considerable thickness and high weight, while their inherent high electromagnetic loss severely impedes the transmission of communication signals [4–7]. In contrast, wave-transmitting materials are engineered to exhibit minimal insertion loss within specific frequency bands. These materials serve a dual purpose: providing physical protection for transmitting antennas and radiation sources against environmental damage, while simultaneously minimizing electromagnetic wave refraction and reflection, thereby ensuring the stable operation of communication systems and electronic devices in complex environments. Nevertheless, their inability to absorb out-of-band interference or probing signals results in a large radar cross-section (RCS) [8,9]. Therefore, there is an urgent need for novel integrated absorption-transmission materials that reconcile wave transmission (for communication) and wave absorption (for stealth), enabling intelligent management of the electromagnetic spectrum [10].

* e-mail: yaolan@dhu.edu.cn

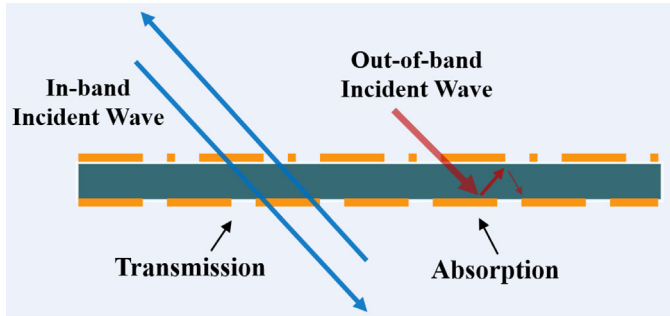


Fig. 1. Typical structure of FSR.

The conceptual basis for integrated absorption and transmission can be traced back to a 1995 patent by W. S. Arceneaux entitled ‘Absorptive/Transmissive Radome’ [11]. This patent qualitatively described a radome structure capable of simultaneous transmission and absorption, characterized by low in-band insertion loss and high out-of-band absorption. Consequently, researchers have progressively broadened their investigations into electromagnetic metamaterials [12–15]. However, the concept did not receive widespread attention due to the lack of sufficiently accurate methods for obtaining material parameters [16,17]. In 2009, Professor Munk proposed an absorber structure with frequency-selective characteristics, which realized the properties of wave absorption outside the operating band and wave transmission within it [18]. Due to this unique functionality, such materials are aptly termed ‘rasorbers’ — a portmanteau of ‘radome’ and ‘absorber’ [19]. The typical structure is shown in Figure 1. However, traditional rasorber structures, which are predominantly fabricated from metallic patterns on rigid dielectric substrates, are limited by their high density, substantial weight, poor corrosion resistance and limited conformability. This restricts their application in lightweight and flexible platforms. To overcome these limitations, the focus of research has shifted towards advanced designs based on resistive film materials and structures [20,21]. Compared to traditional FSRs, the core advantages of resistive film FSRs stem from the inherent properties of resistive film materials and structural innovations. These designs utilize resistive film materials as the core medium for electromagnetic response: resistive films with micron-scale thickness replace traditional lumped-element resistors, enabling broadband absorption through distributed impedance modulation; planar film patterns substitute bulky metal structures, effectively reducing the unit cell period while maintaining resonance characteristics, which suppresses grating lobes and enhances angular stability. Furthermore, leveraging the intrinsic properties of resistive films, these structures produce multifunctional compatibility such as transparency, flexibility, and high-temperature resistance, overcoming the limitations of traditional FSR in scenario adaptation. Beyond the prominent advantages of flexibility, thin-film architectures offer two further critical benefits for advancing FSR performance. First, their fabrication is highly compatible with high-resolution patterning techniques, such as photolithography and laser cutting. This enables the realization of intricate

subwavelength patterns and fine features, which are essential for the drastically reduced unit cell sizes required at higher frequencies—a level of precision challenging to achieve cost-effectively with traditional lumped elements or subtractive metal patterning. Second, the electromagnetic response of resistive films is governed by their tailorable sheet resistance, acting as distributed surface impedance layers. This property allows designers to precisely control the balance between energy dissipation in absorption bands and low insertion loss in transmission bands. In contrast, the performance of traditional metal conductors at these frequencies is increasingly constrained by the skin effect, which leads to higher losses and current crowding. The tailored impedance approach of thin films effectively bypasses these limitations, making them exceptionally suitable for high-performance rasorbers.

This deep coupling of “resistive film material properties – electromagnetic principles – structural design” endows resistive film FSR with unique advantages in ultrathinness, low loss, high integration, and dynamic tuning. Leveraging their lightweight, corrosion resistance, and excellent integrability, thin-film architectures offer an ideal platform for the next generation of integrated absorption-transmission materials [22–24]. The central challenge lies in resolving the fundamental physical challenge between wave absorption and transmission within the confined dimensions of a thin film. This is achieved through the combination of structural design and resistive film materials to precisely allocate electromagnetic energy on demand. However, the growing diversity of resistive films—including carbon-based, indium tin oxide (ITO), and other functional materials—has created a knowledge gap. Existing literature often focuses on individual material types, lacking a unified and comparative perspective that critically assesses the performance frontiers and application-specific advantages of different resistive film families for FSRs.

This article presents a systematic examination of recent advances in resistive film frequency selective absorbers. It commences with the fundamental principles governing the operation of these devices. Subsequently, the discussion is structured around the dominant material systems, providing a detailed analysis of carbon-based resistive film, ITO film, specified sheet resistance film and dynamically tunable resistive film FSRs. For each material category, the review critically examines the design strategies, performance metrics, and the intrinsic link between material properties and device functionality. The article concludes with a forward-looking perspective on the prevailing challenges and promising future research directions in this rapidly evolving field.

2 Fundamental principles of FSR

As an emerging electromagnetic metamaterial, the resistive film frequency selective rasorber (FSR) achieves integrated “out-of-band absorption” and “in-band transmission” functionality through precisely designed periodic structures that manipulate equivalent electromagnetic parameters. This enables the material to exhibit contrasting

electromagnetic responses: low-loss transmission in specified frequency bands and efficient electromagnetic energy dissipation in other spectral regions. While sharing the fundamental operational principles with traditional rasorbers—particularly the reliance on electromagnetic resonance for impedance matching—the incorporation of resistive films introduces unique loss mechanisms that extend beyond conventional design paradigms. These sophisticated structure-property relationships are comprehensively described through the synergistic application of effective medium theory, impedance matching principles, and equivalent circuit models, which collectively establish the critical "structure-parameter-function" relationship specific to resistive film FSRs.

2.1 Effective medium theory

The unit cell of a FSR typically features a subwavelength periodic design, and its overall electromagnetic response can be equivalent to that of a one-dimensional homogeneous and isotropic material. The scattering parameters obtained through electromagnetic simulations can be used to derive the effective permittivity (ε) and effective permeability (μ), which characterize its absorption-transmission properties, thereby providing a quantitative basis for performance control. The transmission matrix T is defined to relate the fields on both sides of the material (Eq. (1)) [14]:

$$T = \begin{pmatrix} \cos(nkd) & -\frac{z}{k}\sin(nkd) \\ -\frac{z}{k}\sin(nkd) & \cos(nkd) \end{pmatrix} \quad (1)$$

where n represents effective refractive index of the material; z represents effective impedance of the material; k represents wave number of the incident electromagnetic wave; d represents material thickness.

Owing to the symmetrical structure of the FSR, a quantitative relationship between the transmission matrix T and the scattering matrix S can be established through electromagnetic theory. The relationship between the simplified S-parameters and the material's electromagnetic parameters is given by equations (2) and (3):

$$S_{11} = S_{22} = \frac{i}{2} \left(z - \frac{1}{z} \right) \sin(nkd) \quad (2)$$

$$S_{21} = S_{12} = \frac{1}{\cos(nkd) - \frac{i}{2} \left(z + \frac{1}{z} \right) \sin(nkd)}. \quad (3)$$

By solving the system of equations simultaneously, the effective refractive index n and effective impedance z of the metamaterial can be determined (Eqs. (4) and (5)).

$$n = \frac{1}{kd} \cos^{-1} \left[\frac{1}{2S_{21}} (1 - S_{11}^2 - S_{21}^2) \right] \quad (4)$$

$$z = \pm \sqrt{\frac{(1 + S_{11})^2 - S_{21}^2}{(1 - S_{11})^2 - S_{21}^2}}. \quad (5)$$

These are related to the effective permeability μ and effective permittivity ε of the metamaterial by: $\mu = nz$, $\varepsilon = \frac{n}{z}$. Consequently, the effective permittivity and effective permeability of the metamaterial can be derived from its simulated S-parameters.

2.2 Impedance matching principle

The core mechanism enabling a rasorber to achieve "out-of-band absorption without reflection and in-band transmission with low loss" is impedance matching. This is realized by tailoring the effective electromagnetic parameters so that the surface impedance of the material matches the impedance of free space, thereby eliminating wave reflection at the interface, while simultaneously dissipating out-of-band energy through dielectric or magnetic loss [25,26]. When an electromagnetic wave is incident normally upon the rasorber, the reflection coefficient R at the interface is determined by the free space impedance Z_0 and the effective impedance of the rasorber Z_R , and can be expressed as:

$$R = \frac{z_R - z_0}{z_R + z_0} \quad (6)$$

where $z_0 = \sqrt{\frac{\mu_0}{\varepsilon_0}}$, $z_R = \sqrt{\frac{\mu_R}{\varepsilon_R}}$, Z_0 represents impedance of free space; Z_R represents effective impedance of the metamaterial; μ_0 represents permeability of free space; ε_0 represents permittivity of free space; μ_R represents effective permeability of the metamaterial; ε_R represents effective permittivity of the metamaterial.

When the effective impedance of the metamaterial matches that of free space ($Z_R = Z_0$), the ratio of the effective permeability to the effective permittivity of the metamaterial becomes equal to that of free space: $\frac{\mu_R}{\varepsilon_R} = \frac{\mu_0}{\varepsilon_0}$. This relationship indicates that the effective permeability and permittivity of the rasorber must maintain a specific, fixed ratio, which forms the fundamental basis for achieving impedance matching within the frequency band.

2.3 Equivalent circuit model

To intuitively describe the electromagnetic response of the rasorber and guide its structural design, each functional layer can be represented by a combination of RLC components and transmission lines [27–30], as shown in Figure 2. This approach allows for the derivation of the overall electromagnetic performance, establishing a quantitative correlation between "structural parameters, circuit parameters, and absorption/transmission performance." A typical dual-layer rasorber can be modeled using an equivalent circuit such as the following:

As illustrated in the figure, Z_{in} and Z_{out} represent the input and output impedance of the metamaterial, respectively. R_1 , L_1 , and C_1 represent the resonance of

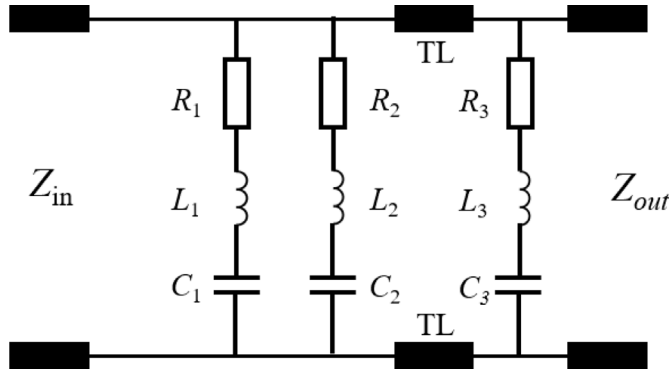


Fig. 2. Equivalent circuit of a dual-layer rasorber.

the top-layer resonant structure; R_2 , L_2 , and C_2 represent the electric dipole resonance of the top-layer resonant structure; M denotes the coupling coefficient between these two resonances; TL represents the dielectric spacer layer between the upper and lower structures; R_3 , L_3 , and C_3 represent the dipole resonance of the bottom-layer structure. Consequently, the transmission-line matrix of the metamaterial can be expressed as (Eq. (7)):

See equation (7) below.

Here, X_1 , X_2 and X_3 can be respectively expressed as:

$$X_1 = \frac{1}{j\omega C_1} + R_1 + j\omega(L_1 - M) \quad (8)$$

$$X_2 = \frac{1}{j\omega C_2 + R_2 + j\omega(L_2 - M)} \quad (9)$$

$$X_3 = \frac{1}{j\omega C_3} + R_3 + j\omega L_3 \quad (10)$$

The scattering matrix S of the metamaterial is obtained by transforming the ABCD matrix (Eq. (11)):

$$\begin{aligned} & \begin{bmatrix} S_{11} & S_{12} \\ S_{21} & S_{22} \end{bmatrix} \\ &= \begin{bmatrix} \frac{AZ_0 + B - (CZ_0 + D)Z_i}{AZ_0 + B + (CZ_0 + D)Z_i} & \frac{2\sqrt{Z_i Z_0}}{AZ_0 + B + (CZ_0 + D)Z_i} \\ \frac{2\sqrt{Z_i Z_0}}{AZ_0 + B + (CZ_0 + D)Z_i} & \frac{-AZ_0 + B - (CZ_0 - D)Z_i}{AZ_0 + B + (CZ_0 + D)Z_i} \end{bmatrix} \end{aligned} \quad (11)$$

The performance of a rasorber is primarily characterized by its out-of-band absorption and in-band transmission properties. The out-of-band absorption rate is determined by the reflectance $R(\omega)$ and transmittance T

(ω), and its absorption of electromagnetic waves can be expressed by the following equation (12):

$$A(\omega) = 1 - R(\omega) - T(\omega) \quad (12)$$

Thus, in an ideal FSR design, the following conditions must be satisfied: in the absorption band, there should be neither reflected nor transmitted waves ($|S_{11}| = 0$ and $|S_{21}| = 0$); whereas in the passband, the incident wave should pass through the structure without loss ($|S_{11}| = 0$ and $|S_{21}| = 1$). In practical applications, the absorption band outside the passband is defined by $S_{11} \leq -10$ dB, while the passband requires $S_{21} \geq -3$ dB.

2.4 Loss mechanism of resistive films

In the design of resistive film FSRs, the resistive film serves as a distributed lossy component whose core parameter—sheet resistance—requires precise optimization to achieve efficient electromagnetic energy conversion. Guided by impedance matching theory, during the absorption band, the coordinated design of the resistive film with dielectric layers and resonant elements enables the structure's equivalent input impedance to approach the free-space impedance (approximately $377 \Omega/\text{sq}$), thereby maximizing energy dissipation. During the transmission band, however, the resonant characteristics of the frequency selective surface (FSS) or sophisticated patterning designs render the resistive film effectively “transparent” to electromagnetic waves, enabling low-loss signal transmission. While the equivalent circuit can be simplified as a lumped-element resistor R , high-frequency applications must account for the RLC resonant network formed by parasitic inductance (L) and capacitance (C), expressed as equation (13):

$$Z_{film} = R + j\omega L + \frac{1}{j\omega C}. \quad (13)$$

These parasitic parameters directly impact high-frequency performance and the feasibility of ultra-broadband designs [31–33]. Furthermore, the patterning of resistive films like cross-shaped and square-loop configurations, provides an effective approach for precisely tailoring the resonant frequency and bandwidth of FSRs by modifying the equivalent inductance and capacitance of the resonant units. Based on the fundamental principles outlined above, the following sections will provide a systematic review of resistive film FSRs organized by material systems. A comprehensive analysis will be presented for four main categories: carbon-based films, ITO film, specified sheet resistance film and dynamically tunable resistive film FSRs. For each category, this review

$$\begin{bmatrix} A & B \\ C & D \end{bmatrix} = \begin{bmatrix} \cos(kl) + \frac{jZ_c \sin(kl)}{X_3} & jZ_c \sin(kl) \\ \left(\frac{1}{\frac{X_1 X_2}{X_1 + X_2} + M} \right) \cos(kl) + \frac{j \sin(kl)}{X_3 Z_c} \left(X_3 + \frac{Z_c^2}{\frac{X_1 X_2}{X_1 + X_2} + M} \right) & \cos(kl) + \frac{jZ_c \sin(kl)}{\frac{X_1 X_2}{X_1 + X_2} + M} \end{bmatrix} \quad (7)$$

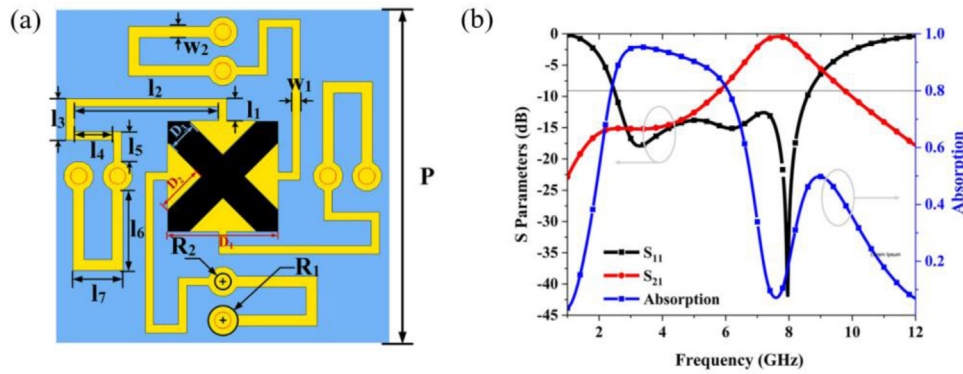


Fig. 3. Miniaturized raserber using graphene films: (a) Lossy layer of FSR. (b) S-parameters under TE polarization [34].

will examine intrinsic material properties, corresponding design methodologies, achieved performance characteristics, and suitability for specific application scenarios. This material-centric approach aims to elucidate the intricate relationships between material selection, structural design, and ultimate device functionality, offering valuable insights for the development of next-generation FSRs.

3 Different materials based resistive film FSRs

Building upon the operational principles detailed previously, the selection of resistive film materials emerges as a critical degree of freedom in tailoring FSRs for specific functionalities. The intrinsic properties of different films—such as electrical conductivity, optical transparency, mechanical flexibility, environmental stability, and tunability—directly govern the ultimate performance limits and application potential of the resulting devices. To elucidate the structure-property-performance relationships, this chapter categorizes resistive film FSRs into four distinct classes for detailed discussion: Carbon-based resistive films, exemplified by graphene and carbon cloth, renowned for their tunable conductivity and flexibility; ITO-based resistive films, centered on indium tin oxide, uniquely combining optical transparency with electromagnetic manipulation; specified sheet resistance films, utilizing ceramics or polymer composites with stable sheet resistance to meet demands in extreme environments like high temperatures and mechanical loading; and dynamically tunable resistive film FSRs, employing materials such as liquid metals and phase-change compounds to pioneer devices with dynamic reconfigurability and cognitive sensing capabilities. This classification framework aims to trace the evolutionary path from material innovation to functional realization, providing a clear roadmap for material selection in resistive film FSR design.

3.1 Carbon-based resistive film FSRs

Carbon-based resistive films, primarily including graphene and carbon cloth, constitute a key material system for constructing absorption-transmission-integrated metamaterials. Their core value lies in their controllable sheet resistance and exceptional flexibility, providing a material

foundation for achieving static to dynamic electromagnetic regulation from microwave to terahertz frequencies. Following an evolutionary logic of functional complexity, this chapter begins by analyzing designs that achieve functional band separation, which respectively realize strong absorption and low-loss transmission in two distinct frequency bands. These designs primarily manifest in two typical spectral forms: low-frequency absorption with high-frequency transmission (A-T), and low-frequency transmission with high-frequency absorption (T-A). Subsequently, the chapter will delve into more complex multi-band management designs, such as A-T-A FSRs with absorption bands on both sides of the transmission band, thereby elucidating the unique role of carbon-based materials in achieving high-performance structural functional devices.

Graphene-based thin films have emerged as preferred materials for ultra-miniaturized A-T FSRs due to their uniform loss characteristics and integration flexibility. Chen et al. [34] employed a cross-shaped graphene pattern with a sheet resistance of $360 \Omega/\text{sq}$ as the core lossy layer, combined with metal vias and meander lines to construct a 2.5D structure, which is shown in Figure 3a. The vias connect copper patches on the upper and lower surfaces of the lossy layer, effectively utilizing the three-dimensional space to compress the unit cell period to $0.05\lambda_L$ (where λ_L is the wavelength at the lowest absorption frequency). This design successfully suppresses grating lobes, enabling the device to maintain a -10 dB reflection bandwidth (absorption rate $>80\%$) from 2.54 to 8.58 GHz and a transmission band (insertion loss ≈ 0.26 dB) from 7.27 to 8.01 GHz, even at oblique incidence angles up to 50° (Fig. 3b). This performance makes it suitable for applications such as bistatic stealth radomes. Wu et al. [35] further optimized the graphene-based structure by introducing multiple via-connected metal stubs to generate dense resonance points. This configuration reduced the unit period to $0.039\lambda_L$ and the total thickness to merely $0.076\lambda_L$. The resulting design achieves an ultra-wide absorption band from 1.96 to 10.2 GHz (fractional bandwidth of 135.5%) and a low-loss transmission band from 12.02 to 13.55 GHz (insertion loss <1 dB), while maintaining stable performance under oblique incidence up to 45° . These advancements meet the low-profile requirements of miniaturized stealth devices.

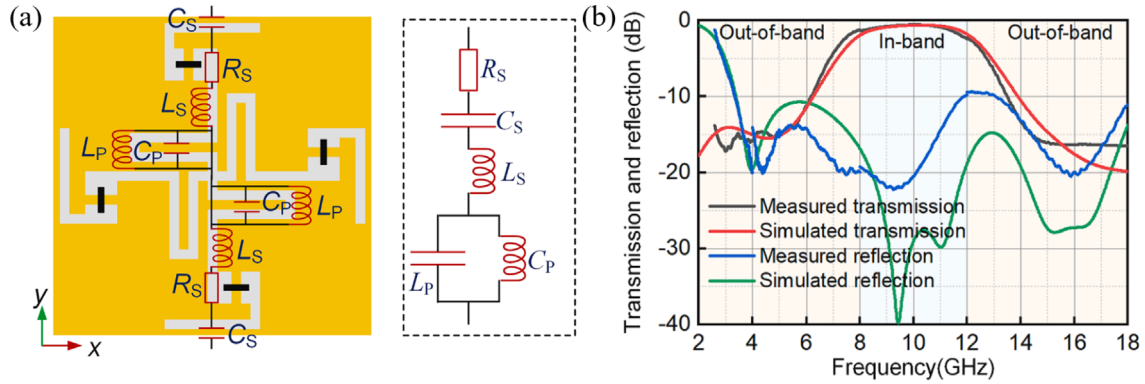


Fig. 4. Carbon film FSR with out-of-band absorption and in-band transmission: (a) Structure of lossy layer in FSR. (b) Electromagnetic properties of FSR [39].

The aforementioned work primarily enhances performance through three-dimensional structural optimization. However, by integrating graphene with other functional layers or resonant structures to construct hybrid architectures, more precise manipulation of the spectral response can be achieved, such as expanding the low-frequency transmission bandwidth or sharpening the transmission band edges.

Then, Pang et al. [36] innovatively employed multi-layer graphene to design a dual-lossy-layer structure integrated with a capacitive metasurface. This configuration achieved low-loss transmission below 1 GHz and ultra-wideband absorption from 3.6 to 14 GHz. The uniform loss characteristics of graphene eliminated soldering errors associated with lumped elements, significantly enhancing process reliability. Mao et al. [37] innovatively proposed a graphene-based rasorber, which adopts a cascaded configuration of a lossy layer with graphene ohmic sheet-configured Jerusalem cross and a second-order bandpass frequency selective surface (FSS) as the bottom layer. This design realized low-loss transmission in the X band (9.36–11.8 GHz under 1 dB insertion loss) and ultra-wideband absorption in the Ku band (13.2–18 GHz under -10 dB reflection), while narrowing the transitional band between the transmission and absorption bands to 1.4 GHz. The planar structure of graphene eliminated soldering errors associated with lumped elements, and the transmission zero introduced by the FSS sharpened the passband edge to reduce the transitional band.

Hybrid architectures demonstrate the potential for achieving excellent performance in dual bands. Extending the design objective from two functional bands to three or more, i.e., achieving multi-band management, places higher demands on material and structural design, often requiring simultaneous consideration of the device's mechanical properties or flexibility. Yin et al. [38] achieved a breakthrough using multi-layer graphene and via-wound inductors: the graphene film ensured wideband loss, while the via-wound inductors broadened the transmission band. The final design achieved ultra-wideband impedance matching from 1.56 to 18 GHz, a transmission band from 7.15 to 12.4 GHz with a minimum insertion loss of 0.56 dB, and absorption rates $\geq 80\%$ in the 1.4–5.4 GHz and 13.6–18 GHz bands, making it suitable for ultra-wideband radar stealth and communication. Yang et al. [39] proposed a

foam-core sandwich structure, fabricating a carbon film FSR composite using epoxy film and VARTM processes. The lossy layer is shown in Figure 4a and the electromagnetic properties is shown in Figure 4b. The structure achieved absorption rates $\geq 80\%$ in 3.2–6.4 GHz and 13.2–18 GHz, transmission rates $\geq 80\%$ in 9–11.3 GHz, a flexural strength ≥ 35 MPa, and a compressive modulus ≥ 49 MPa, marking the first realization of A-T-A FSR with integrated mechanical and electromagnetic properties. Besides, Yang et al. [40] embedded PIN diodes within a quartz fiber/PMI foam composite structure, and also introduced carbon-based films by screen-printing at the reserved gaps of copper patterns to assist in achieving stable out-of-band absorption. This design achieved a bending modulus of 938.4 MPa, resolving the industry challenge of mechanical fragility in tunable devices.

Chen et al. [41] designed an all-textile A-T-A FSR, using a nylon substrate for the top layer, carbon cloth (sheet resistance $250 \Omega/\text{sq}$) as the lossy layer, and copper cloth to form an ELC resonator, resulting in a flexible film based FSR, which is shown in Figure 5a. It achieved absorption rates $\geq 80\%$ in 1.35–2.2 GHz / 3.05–4.1 GHz, transmission rates of 86% at 2.59 GHz (Fig. 5b), and the carbon cloth sheet resistance deviation remained $< 10\%$ after two laundering cycles, filling a gap in the field of flexible FSRs.

Meanwhile, in fields like aerospace, structural lightweighting without compromising performance remains a core and challenging objective. Han et al. [42] employed aramid paper honeycomb as the supporting structure, developing two configurations using commercial absorbing films and carbon paste slot-line circuits, respectively. Among them, the carbon paste circuit structure forms an absorption channel by printing carbon paste with a sheet resistance of $80 \Omega/\text{sq}$ at the four corners of the aramid-paper honeycomb cell. This structure achieves a passband insertion loss as low as 0.7 dB at the center frequency of 7 GHz, and dual absorption bands are formed on the lower and upper sides of the passband 3–5 GHz and 9–12 GHz with an absorption more than 90% for both bands. These designs achieved an areal density of $< 200 \text{ g}/\text{m}^2$, representing a 60% weight reduction compared to traditional metal FSRs, thereby addressing the integration challenge of “high load-bearing, lightweight, and electromagnetic stealth”.

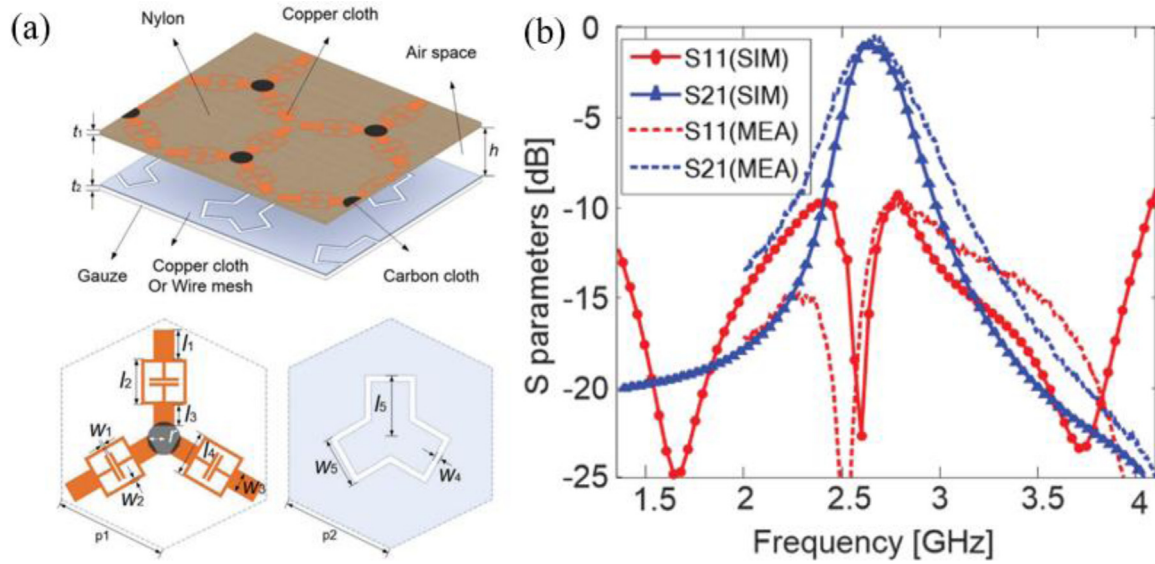


Fig. 5. All-fabric flexible FSR: (a) Unit cell of FSR. (b) S-parameters [41].

Carbon-based resistive films, through their tunable and easily integrable characteristics, provide design flexibility for frequency selective absorbers. This integrability is practically enabled by versatile fabrication methods. Low-cost, scalable techniques like screen printing of carbon pastes or graphene inks facilitate high-throughput production on both rigid and flexible substrates, while laser cutting offers a high-precision alternative for applications demanding superior pattern fidelity. This foundation in manufacturability enables functionality ranging from single-band to multi-band absorption-transmission manipulation. The evolution of single-band designs demonstrates that three-dimensional configurations and hybrid architectures can effectively address the challenge of synergizing broadband absorption with low-loss transmission. The realization of multi-band absorption-transmission functionality marks a new phase in the development of carbon-based materials, transitioning from purely electromagnetic devices to structural-functional integration and flexible applications. Current challenges lie in further enhancing the dynamic tuning speed and stability of graphene-based devices, as well as optimizing the process robustness of large-area flexible structures. Research addressing these issues will establish a foundation for carbon-based materials to function effectively in broader application scenarios.

3.2 ITO-based resistive film FSRs

Following carbon-based films, Indium Tin Oxide (ITO) films, as another key material class, have opened new avenues for absorption-transmission-integrated metamaterials, leveraging their unique optical transparency and tunable conductivity. The electrical and optical properties of ITO films are predominantly determined during the deposition process, with key parameters including film thickness, doping concentration, and post-annealing con-

ditions, which collectively govern the trade-off between sheet resistance and visible light transmittance. For FSR designers, these intrinsic material characteristics translate into critical design degrees of freedom: the sheet resistance directly influences the absorption efficiency and bandwidth, while the optical transmittance determines the suitability for transparent applications. Unlike carbon-based materials, ITO films enable effective microwave and millimeter-wave management without significantly compromising visible light transmission. This characteristic renders them irreplaceable in scenarios requiring both visual and electromagnetic functionalities, such as transparent radomes and smart windows. This chapter will systematically elucidate the design strategies of ITO-based integrated metamaterials, focusing on their evolution from static to dynamically tunable functions, and from rigid substrates to flexible transparent devices.

Leveraging their optical transparency and controllable conductivity, ITO films have expanded the functional boundaries FSRs. Deng et al. [43] designed a structure centered on ITO, featuring a “cross-shaped interdigital lossy layer – quartz glass spacer layer – square loop FSS layer”, as shown in Figure 6a. The ITO absorption layer, with a sheet resistance of $10 \Omega/\text{sq}$, achieves above 90% absorption in the X-Ku band (7.7–18.4 GHz) through series resonance. The ITO transmission layer, with a sheet resistance of $1 \Omega/\text{sq}$, enables transmission in the Ka band (26.7–29.4 GHz) with an insertion loss of approximately 1.2 dB (Fig. 6b). Concurrently, the quartz glass substrate synergizes with the ITO to ensure a visible light transmittance of 76.9%. This work marks the first realization of A-T characteristics compatible with “transparency and millimeter-wave transmission”, making it suitable for applications such as transparent radomes and automotive windows. In a separate approach, Yi et al. [44] incorporated ITO films into a waveguide system. They fabricated periodic slits on a 500 nm-thick ITO film via

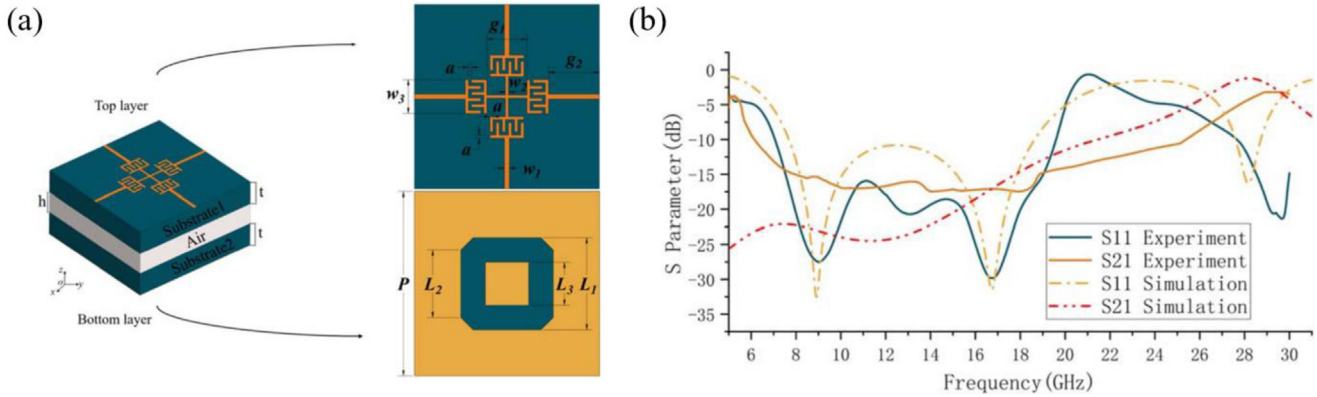


Fig. 6. A compact optical transparency FSR: (a) Schematic diagrams of FSR. (b) S-parameters [43].

laser etching and embedded it on a glass substrate within a rectangular waveguide. This strategy breaks through the conventional free-space application limitations of FSRs and offers a new solution for electromagnetic shielding in waveguides.

The aforementioned research established the foundation for ITO films in achieving static, fixed-band functionality. However, modern multifunctional systems often require flexible combinations of absorption-transmission characteristics across different frequency bands, placing higher demands on the multi-band compatibility of devices. Lin et al. [45] proposed two lumped-element-free designs: Structure I, featuring an ITO cross-shaped lossy layer, achieved absorption from 7.94 to 12.4 GHz and transmission from 2.36 to 2.78 GHz; Structure II, utilizing a sector-ring lossy layer, provided absorption from 9.41 to 17.48 GHz and transmission from 26.90 to 27.34 GHz, catering to diverse communication-stealth requirements across different bands (Fig. 7).

Achieving multi-band compatibility is a significant step in functional evolution, yet endowing devices with dynamic tunability is key to developing “smart” electromagnetic metasurfaces. The functional flexibility of ITO-based structures can be significantly enhanced through the integration of active components. Fan et al. [46] embedded varactor diodes into square-loop metal patterns, enabling continuous tuning of the transmission window from 1.8 to 4.5 GHz by applying a 0–15 V reverse bias voltage, while achieving >10 dB RCS reduction from 5.4 to 14.1 GHz. Integrating an ITO-based infrared stealth layer, this work marked the first realization of multi-spectral compatibility encompassing “radar-infrared-frequency hopping communication”, which will address the subject of radome applications. Besides, Utilizing the intrinsic physical properties of materials to achieve functional state switching represents a concise and efficient strategy towards dynamic control. Modulation based on the dielectric properties of liquids is one such example. Kong et al. [47] adopted a novel approach by designing a liquid reconfigurable stealth window that consists of an anti-reflection glass with indium tin oxide (ITO) as resistive film and a PMMA transparent container filled with ethanol, leveraging the dielectric property contrast of the liquid for state switching: drainage enabled low-loss transmission

from 2.3 to 5 GHz, while filling the container achieved over 90% absorption from 4.5 to 10.5 GHz, alongside a visible light transmittance of 80.3% (Fig. 8). Subsequently, active tunability emerged as a core technological direction.

Tunable designs significantly expand the application dimensions. Furthermore, integrating devices with flexible substrates can meet the requirements of conformal carrier platforms. Recently, ITO films have also demonstrated great potential in the field of flexible transparent devices. In 2024, targeting flexible conformal carriers, Ma et al. [48] utilized ITO-PET films and PVC flexible substrates, realizing for the first time a T-A type FSR integrating “flexibility, transparency, and ultra-wideband” characteristics. Conversely, focusing on aerospace heavy-load scenarios (Fig. 9).

As device structures and functional requirements become increasingly complex, traditional trial-and-error design methods face efficiency bottlenecks. Data-driven inverse design offers a new paradigm to address this challenge. Similarly, in terms of design methodology innovation, Sun et al. [49] discretized the lossy layer into an 8×8 binary-coded sub-array. By employing an Improved Estimation Distribution Algorithm (IEDA) to optimize the coding pattern, ITO sheet resistance, and layer thickness, the optimized design achieved wide transmission from 0 to 5.44 GHz ($|S_{21}| > -3$ dB) and high absorption from 8.30 to 18.62 GHz (absorption rate > 90%). This data-driven inverse design approach reduced the development cycle by 60% compared to traditional trial-and-error methods, effectively eliminating reliance on empirical intuition.

ITO-based resistive film has successfully combined optical transparency with effective electromagnetic manipulation capabilities, giving rise to FSR devices suitable for transparent window scenarios. These capabilities are enabled by sophisticated fabrication processes, primarily magnetron sputtering for depositing high-quality ITO films and laser cutting for precise patterning of FSS structures. While sputtering ensures excellent film uniformity, its vacuum-based nature significantly contributes to fabrication costs, and laser cutting’s precision is crucial for maintaining high-frequency performance by avoiding edge defects. Through elaborate multi-layer structures and pattern designs, multi-band compatibility and dynamic

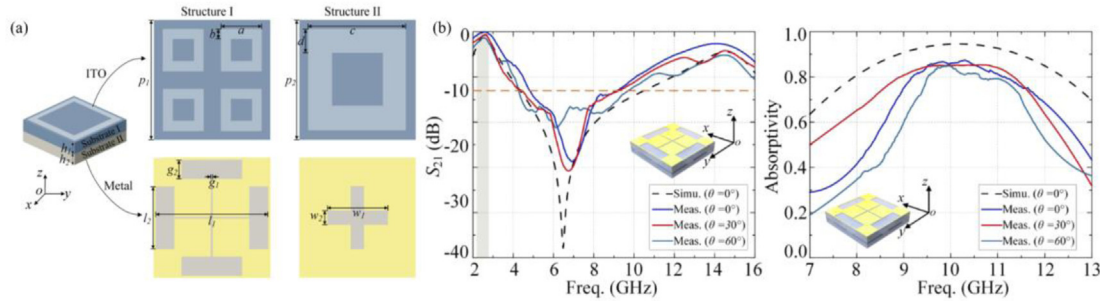


Fig. 7. FSR based on customizable impedance films: (a) Two structures of FSR. (b) Electromagnetic properties [45].

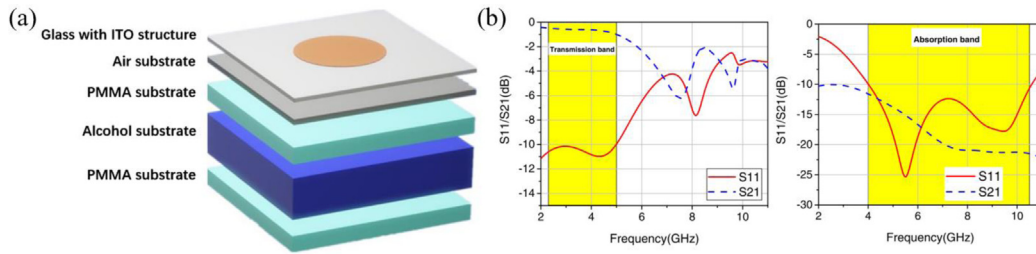


Fig. 8. A liquid reconfigurable FSR: (a) Basic composition schematic of a single unit cell. (b) S-parameters with and without ethanol [47].

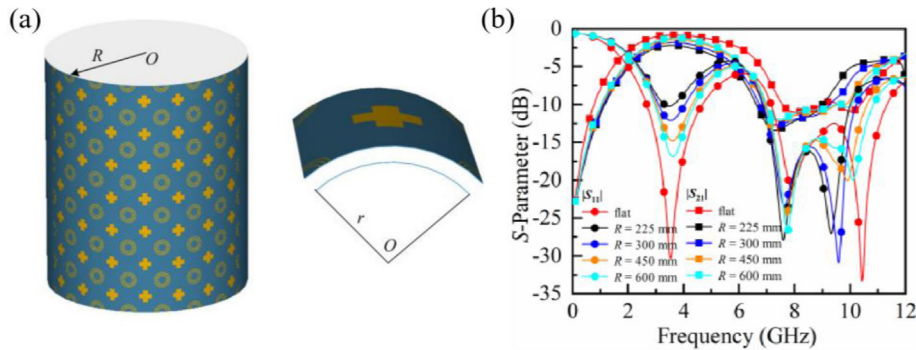


Fig. 9. A flexible and transparent FSR: (a) Curved unit cell of the proposed flexible FSR [48]. (b) S-parameters of FSR [48].

tunability have been achieved, significantly enhancing the situational adaptability of the devices. Furthermore, flexible devices based on ITO-PET demonstrate potential for application on conformal platforms. At the design methodology level, the introduction of inverse design algorithms signifies a transition from experience-driven to intelligent design in this field. Currently, the development of ITO-based integrated materials still faces challenges such as sheet resistance uniformity, the cost of large-area fabrication, and the long-term stability of integration with flexible substrates. Future research is expected to make breakthroughs in these areas.

3.3 Specified sheet resistance film FSRs

Beyond carbon-based and ITO films, a range of specified sheet resistance films, leveraging their unique physical properties—such as high-temperature resistance and reconfigurability—provide innovative solutions for absorp-

tion-transmission-integrated metamaterials in extreme environments, special frequency bands, and dynamic scenarios. This chapter focuses on these material systems designed for specific demands. Following an evolutionary logic of functionality, it progresses from designs achieving single-band function separation (A-T/T-A) to devices enabling complex multi-band management (A-T-A), systematically elucidating their prominent value in expanding the application boundaries of integrated technology.

For extreme high-temperature environments, An et al. [50] proposed an integrated design incorporating a patterned resistor film (PRF) with a ceramic substrate, which is shown in Figure 10. The PRF, with a sheet resistance of $100 \Omega/\text{sq}$, was printed as the lossy layer onto a SiO_2 fiber paper. The resulting device maintains an absorption rate $> 80\%$ within the 5.1–12.6 GHz frequency band, and exhibits an insertion loss $< 3 \text{ dB}$ in the 15.5–15.8 GHz band, while simultaneously achieving a bending

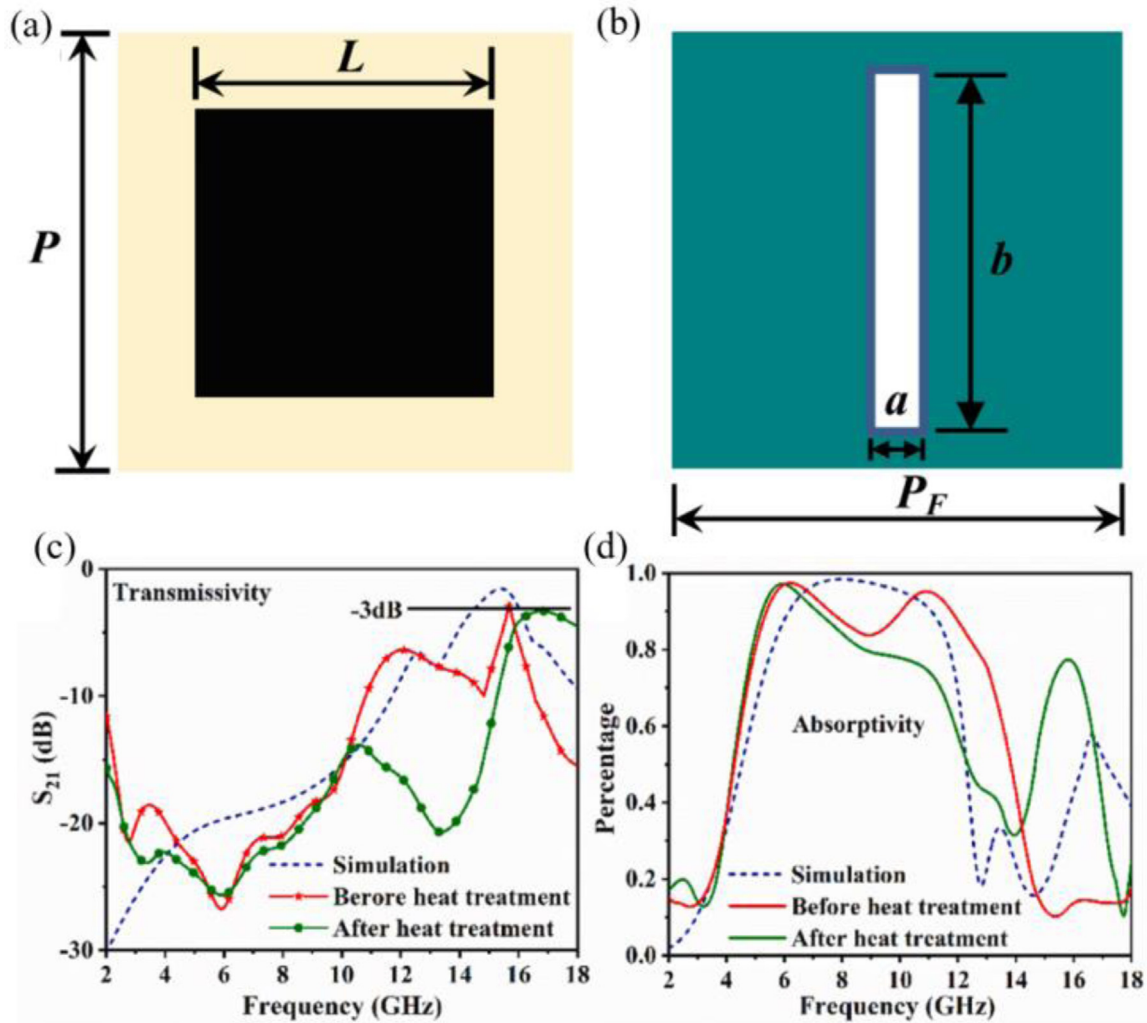


Fig. 10. A high temperature resistance FSR with PRF: (a) Lossy layer structure and (b) FSS layer of FSR. (c) Transmissivity and (d) Absorptivity of FSR [50].

strength of 43.9 MPa. This addresses the critical challenge of integrating high-temperature load-bearing capacity with stealth functionality in radomes for hypersonic vehicles.

While material innovations for extreme environments address device survivability, methodological revolutions in design aim to enhance device performance and optimize the development process. Data-driven design based on coding metasurfaces offers an effective pathway to this goal. Zhang et al. [51] utilized a high-impedance resistor film (sheet resistance 226.5 Ω /sq) as the lossy layer and innovatively adopted a discrete coding meta-surface design strategy, which is shown in Figure 11a. This approach ultimately realized an absorption band from 2.18 to 6.14 GHz (absorption rate > 80%) and a transmission band from 6.88 to 12.94 GHz (insertion loss < 3 dB), with a transition band of only 0.74 GHz, while maintaining compatibility with dual polarizations (Fig. 11b). This methodology shifts the design paradigm for A-T type FSRs from “experience-driven” to “data-driven,” reducing the development cycle by approximately 50% compared to traditional trial-and-error methods.

Building upon the basic A-T functionality, refining the spectral response—such as suppressing harmonics and expanding bandwidth—is crucial for enhancing device practicality. In 2020, Yu et al. [52] utilized a square resistor film combined with a metal square-loop FSS to construct a structure exhibiting a main passband centered at 8 GHz. This design effectively suppressed harmonic transmission windows and absorbed out-of-band reflection from 12 to 26 GHz. Lightweight design addresses the load-bearing requirements of macro-structures. At the micro-fabrication level, developing low-cost, high-consistency integration processes is crucial for advancing device practicality. Zhou et al. [53] proposed replacing lumped-element resistors with screen-printed resistive ink in a double-layer structure. Experimental results demonstrated absorption rates $\geq 80\%$ in the 3.5–9.3 GHz and 11–15.8 GHz bands, with a minimum insertion loss of only 0.47 dB in the 9.7–10.5 GHz band. Since the resistive ink requires no soldering and its sheet resistance can be flexibly adjusted, the process cost was reduced by 40% compared to the lumped-element resistor solution. Wan et al. [54] addressed the polarization

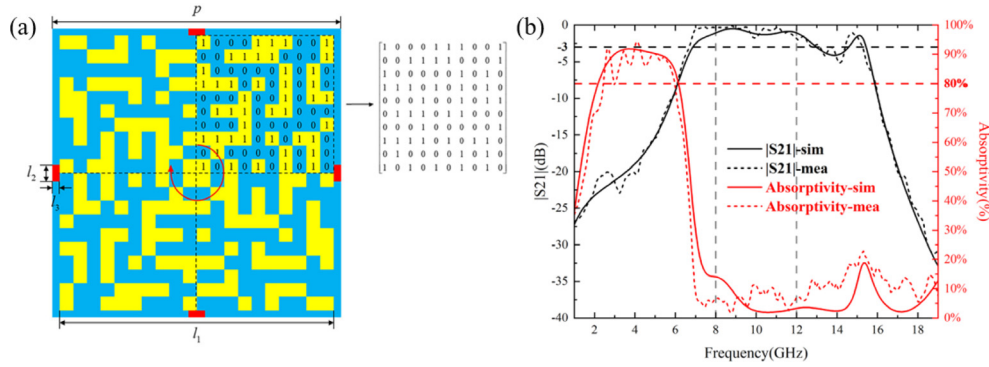


Fig. 11. A dual-polarized broadband FSR: (a) The coding structure of FSR. (b) S-parameters [51].

sensitivity of traditional FSRs using a chiral absorber and a C_4 -symmetric structure. They designed an absorptive split-ring resonator (ASRR) incorporating a resistive film, achieving absorption in the 1.5–3.6 GHz and 15.2–21.6 GHz bands and transmission in the 8–12 GHz band. Measurements showed an absorption rate deviation of $<5\%$ under arbitrary polarization incidence and excellent angular stability up to 45° , making it suitable for multi-polarization radar systems.

The various specified sheet resistance films discussed in this section demonstrate the diversity and innovativeness of integrated technology in addressing specific application challenges. These capabilities are supported by mature fabrication strategies that effectively combine additive processes like screen printing for applying resistive pastes with subtractive methods like PCB etching for patterning metallic components. At the single-band function separation level, breakthroughs ranging from extreme environment adaptability to design methodology revolution have been achieved through means such as high-temperature ceramic integration and coding metasurface design. At the multi-band management level, these fabrication approaches, particularly the low-cost nature of screen printing and the precision of PCB etching that enables component integration, have successfully advanced device functionality to new heights in low-cost manufacturing and polarization insensitivity. Collectively, these studies indicate that material innovation, structural design, and their corresponding fabrication methodologies tailored to specific demands are the core drivers continuously propelling the development of absorption-transmission-integrated metamaterials.

3.4 Dynamically tunable resistive film FSRs

Beyond the static performance offered by conventional resistive films, the frontier of FSR research is advancing towards dynamic adaptability. This subsection focuses on dynamically tunable resistive film FSRs, a category characterized by their ability to actively or passively reconfigure electromagnetic responses based on external stimuli or operational frequency. By integrating functional materials whose electromagnetic properties can be intentionally altered—such as liquid metals and phase-change

materials—these devices transcend fixed spectral functionalities, paving the way for intelligent, situation-aware electromagnetic systems.

Achieving high-performance static multi-band management is a significant milestone. However, endowing devices with the ability to dynamically reconfigure between different functional modes is the core of next-generation adaptive stealth technology. Kong et al. [55] developed a reconfigurable scheme based on the fluidity of liquid metal, addressing the need for dynamic stealth in FSRs. The device integrated two lossy layers and a reconfigurable third-order bandpass FSS, which was constructed by creating grid microchannels on a PMMA substrate. The operating mode is switched by mechanically injecting or withdrawing the EGaIn into/from the microchannels. When the microchannels are filled, the FSS acts as a perfect electric conductor, switching the FSR to the A-R-A mode; when the liquid metal is withdrawn, the intrinsic bandpass response of the FSS is restored, enabling the A-T-A mode. This fluidic actuation mechanism, while resulting in a relatively slow switching speed (on the order of seconds), offers high energy efficiency as no power is required to maintain either state, and promises excellent cyclability due to the inherent self-healing property and minimal degradation of the liquid metal. In A-T-A mode, absorption was $\geq 80\%$ in 5.9–9.5 GHz / 16.2–24 GHz, and the transmission band from 10.1 to 15.6 GHz had a relative bandwidth of 42.8%. In A-R-A mode, the reflection echo loss was <3 dB in the 10.1–15.6 GHz band, adaptable for switchable stealth radomes.

Dynamic reconfiguration technology significantly enhances tactical flexibility in the microwave band. Concurrently, extending the integrated concept to higher frequency bands, such as the terahertz (THz) regime, opens up new research frontiers. In the terahertz (THz) frequency range, Wang et al. [56] designed a three-layer structure specifically for THz applications, utilizing VO_2 phase-change films and resistive films, as shown in Figure 12. The functionality is dynamically switched via thermal control (around 340 K), which triggers the insulator-to-metal phase transition of VO_2 . This thermal switching mechanism exhibits a typical response speed on the order of milliseconds to seconds and demonstrates excellent cyclability (often exceeding 10^5 cycles), though its operation requires sustained energy input to both trigger

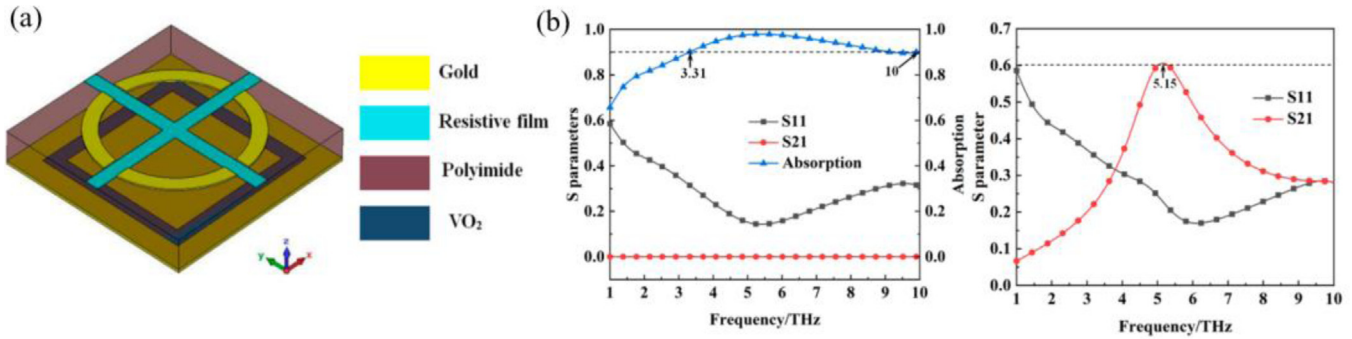


Fig. 12. A multifunctional THz band FSR: (a) Unit cell of FSR. (b) S-parameters [56].

and maintain the phase transition in VO₂. When VO₂ is in a high-conductivity (2×10^5 S/m) metallic state, the bottom layer acts as a metal ground plane, and the structure achieves ultra-wideband absorption greater than 90% from 3.31 to 10 THz, with a relative bandwidth of 100.5%, primarily due to electromagnetic resonance and impedance matching. When VO₂ is in a low-conductivity (10 S/m) insulating state, the bottom layer functions as a frequency-selective surface, creating a transmission peak of 61% at 5.15 THz, which lies within the original absorption band. The device is also insensitive to polarization and maintains its performance for incident angles up to 60°, demonstrating excellent angular stability. This work represents the first realization of a thermally induced dynamic absorption/transmission switching functionality in the THz band. The unique “in-band transmission” characteristic offers a novel solution to integrating communication windows within a broadband stealth platform, addressing a key challenge in THz multi-spectral stealth.

The integration of dynamically tunable resistive films with functional materials like liquid metals and phase-change substances represents a paradigm shift from static designs to truly dynamic systems. However, this shift introduces unprecedented fabrication complexity, requiring hybrid manufacturing approaches that combine techniques like laser cutting for microfluidic channels with vacuum-based deposition for phase-change films. The fundamental principle of this advancement is the successful integration of reconfigurability and frequency-awareness directly into the material system and its manufacturing architecture. These developments not only provide viable solutions for current switchable stealth and multi-spectral compatibility challenges but also lay the foundational material and architectural groundwork for the future realization of fully cognitive electromagnetic surfaces. The current scalability and cost-effectiveness of these sophisticated fabrication processes remain the primary challenge that must be overcome to enable surfaces that can autonomously adapt to complex and changing spectral environments.

4 Material system of resistive films and future prospects

As demonstrated in the preceding exposition on different materials of resistive film FSRs, the applications of carbon-based film, indium tin oxide (ITO) film, specified sheet

resistance film, and dynamically tunable resistive film FSRs in absorption-transmission-integrated metamaterials have been methodically arranged (Tab. 1). Across these material systems, the development follows a clear function-oriented logic: Carbon-based materials dominate in broadband absorption and flexible devices by leveraging their tunable conductivity and flexibility; ITO films define the standard for transparent electromagnetic window applications through their unique optical transparency; while other functional films demonstrate immense potential for customization, targeting specific needs such as high-temperature resistance and dynamic reconfiguration. Despite their differences, the core design philosophy consistently involves the precise control of the sheet impedance of the resistive film and its co-optimization with macroscopic electromagnetic structures, ultimately achieving desired absorption-transmission functionality in classic spectral configurations such as A-T, T-A, and A-T-A.

Current research on resistive film FSRs has successfully addressed frequency band management ranging from dual-band to triple-band configurations, which is shown in Figure 13. Future breakthroughs will focus on leveraging the dynamic properties of materials to achieve real-time, reconfigurable control over these functional modes and further extend to more complex spectral relationships, such as multi-band architectures like Transmission-Absorption-Transmission (T-A-T) or more absorption and transmission bands. This demands that materials possess not only static electromagnetic parameters but also controllable abrupt changes in properties under external stimuli (electrical, thermal, optical, mechanical), such as the insulator-to-metal transition in phase-change materials like VO₂ and the fluidic-to-patterned switching in liquid metals like EGaIn, laying the groundwork for truly adaptive “intelligent spectrum shapers”.

In the future, emerging materials will inject new vitality into integrated absorption-transmission technology. MXene, with its high electrical conductivity, hydrophilicity, and rich surface chemistry, can be easily processed into high-performance transparent electrodes or free-standing films, showing great promise in balancing optical transparency and microwave manipulation. Nanocellulose conductive films, derived from renewable resources, offer properties like biodegradability, ultra-flexibility, and intrinsic transparency. When composited with conductive nanomaterials, they are expected to open new application paradigms in green electronics, temporary implantable

Table 1. Comparison of different resistive film material systems for FSRs.

Material system	Core advantages	Main limitations	Application & typical performance	References
Carbon-based film FSR	Excellent flexibility Tunable conductivity Low-cost fabrication	Moderate processing accuracy	Ultra-wideband Radar Stealth: Absorption bandwidth up to 135% Flexible/Wearable Devices: Stable performance under bending	[34–42]
ITO film FSR	Optical Transparency Good sheet resistance control Smooth surface for high-frequency patterns	Brittleness High cost of material and fabrication	Transparent Radomes: X-Ku band absorption with >76% transmittance Conformal Windows: Flexible ITO/PET for curved surfaces	[43–49]
Specified sheet resistance film FSR	Environmental Robustness Design-specific resistance values Low-cost manufacturing	Limited intrinsic functionality	High-Temperature Radomes: Stable at >1000 °C with 43.9 MPa strength Cost-Sensitive Mass Production: Screen-printed circuits with <3 dB IL	[50–54]
Dynamically tunable resistive film FSR	Reconfigurable Functionality Adaptive response to stimuli Enables cognitive systems	Fabrication Complexity High cost and immature processes	Switchable Stealth Radomes: ATA/ARA mode switching with 42.8% FBW THz Multi-spectral Control: >90% absorption from 3.31–10 THz	[55,56]

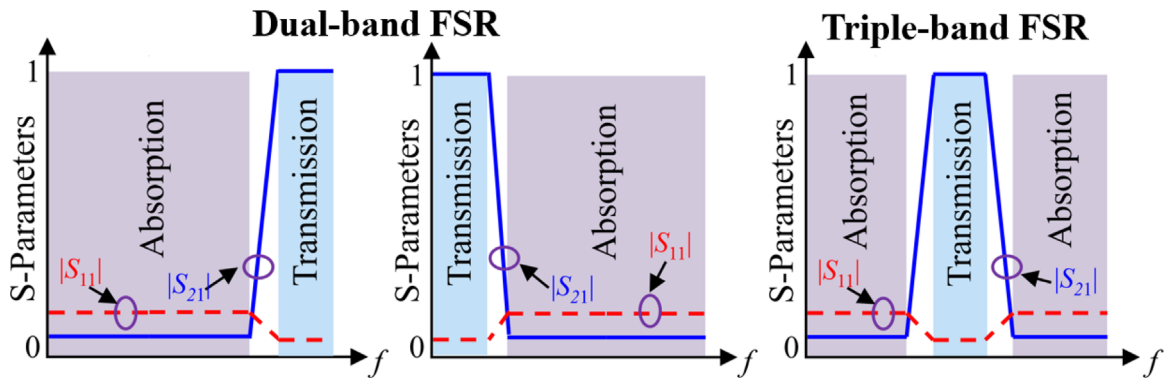


Fig. 13. Frequency band configuration of FSRs.

devices, and environmentally friendly flexible systems. These materials, together with the continuously optimized carbon-based and ITO systems, will collectively propel absorption-transmission-integrated metamaterials towards greater intelligence, integration, and environmental adaptability.

5 Conclusion

This review systematically traces the research progress of resistive film frequency-selective absorbers (FSRs) from the perspective of material systems. Commencing with an elucidation of their fundamental operating mechanisms, it subsequently devotes dedicated sections to dissecting the design paradigms, performance metrics, and application scenarios of carbon-based film, indium tin oxide (ITO) film, specified sheet resistance film and dynamically tunable resistive film FSRs. Special emphasis is placed on elaborating on their commonalities, distinct characteristics, and respective advantages, while explicitly clarifying the pivotal role of intrinsic material properties in dictating FSR device functionality. Through summarizing existing achievements and analyzing future trends, this article indicates that by deepening material innovation, developing dynamic reconfigurable technologies, and integrating with AI-driven design, resistive film integrated metamaterials will continue to push performance boundaries and play an increasingly critical role in future communications, adaptive stealth, and intelligent sensing.

Funding

This work was funded by the “Scientific Research Capacity Enhancement Project of Donghua University”.

Conflicts of interest

The authors have nothing to disclose.

Data availability statement

This article has no associated data generated and analyzed.

Author contribution statement

Jiahua Yang conceived, organized the writing of the article. Kun Zhang guided the writing approach. Lan Yao reviewed all the chapters.

References

1. F. Shahzad, M. Alhabeab, C. B. Hatter, B. Anasori, S. Man Hong, C. M. Koo, Y. Gogotsi, Electromagnetic interference shielding with 2D transition metal carbides (MXenes), *Science* **353**, 1137 (2016), <https://doi.org/10.1126/science.aag2421>
2. R.K. Mishra, R.D. Gupta, S. Datar, Metamaterial microwave absorber (MMA) for electromagnetic interference (EMI) shielding in X-band, *Plasmonics* **16**, 2061 (2021), <https://doi.org/10.1007/s11468-021-01465-y>
3. H. Li, M. Fu, Evaluation and suppression of high-frequency radiated EMI in inductive power transfer system, *IEEE Trans. Power Electron.* **39**, 8998 (2024), <https://doi.org/10.1109/TPEL.2024.3388573>
4. Z.R. Jia, D. Lan, K.J. Lin, M. Qin, K.C. Kou, G.L. Wu, H.J. Wu, Progress in low-frequency microwave absorbing materials, *J. Mater. Sci. Mater. Electron.* **29**, 17122 (2018), <https://doi.org/10.1007/s10854-018-9909-z>
5. J.L. Liu, L.M. Zhang, H.J. Wu, Electromagnetic wave-absorbing performance of carbons, carbides, oxides, ferrites and sulfides: review and perspective, *J. Phys. D Appl. Phys.* **54**, 203001 (2021), <https://doi.org/10.1088/1361-6463/abe26d>
6. M. Qin, L.M. Zhang, H.J. Wu, Dielectric loss mechanism in electromagnetic wave absorbing materials, *Adv. Sci.* **9**, 2105553 (2022), <https://doi.org/10.1002/advs.202105553>
7. L. Xia, Y. Feng, B. Zhao, Intrinsic mechanism and multi-physics analysis of electromagnetic wave absorbing materials: new horizons and breakthrough, *J. Mater. Sci. Technol.* **130**, 136 (2022), <https://doi.org/10.1016/j.jmst.2022.05.010>
8. C. Huang, C. Ji, X.Y. Wu, J.K. Song, X.G. Luo, Combining FSS and EBG surfaces for high-efficiency transmission and low-scattering properties, *IEEE Trans. Antennas Propag.* **66**, 1628 (2018), <https://doi.org/10.1109/TAP.2018.2790430>
9. A.A. Omar, H. Huang, Z.X. Shen, Absorptive frequency-selective reflection/transmission structures: a review and future perspectives, *IEEE Antennas Propag. Mag.* **62**, 62 (2020), <https://doi.org/10.1109/MAP.2019.2943302>
10. R. Panwar, J.R. Lee, Progress in frequency selective surface-based smart electromagnetic structures: a critical review, *Aerosp. Sci. Technol.* **66**, 216 (2017), <https://doi.org/10.1016/j.ast.2017.03.006>
11. W.S. Arceneaux, R.D. Akins, W.B. May, Absorptive/transmissive radome, US Patent, 1995
12. D.R. Smith, D. Schurig, M. Rosenbluth, S. Schultz, J.B. Pendry, Limitations on subdiffraction imaging with a negative refractive index slab, *Appl. Phys. Lett.* **82**, 1506 (2003), <https://doi.org/10.1063/1.1557820>
13. D.R. Smith, J.B. Pendry, M.C.K. Wiltshire, Metamaterials and negative refractive index, *Science* **305**, 788 (2004), <https://doi.org/10.1126/science.1096796>
14. J.B. Pendry, D. Schurig, D.R. Smith, Controlling electromagnetic fields, *Science* **312**, 1780 (2006), <https://doi.org/10.1126/science.1125907>
15. D.R. Smith, J.B. Pendry, Homogenization of metamaterials by field averaging, *J. Opt. Soc. Am. B* **23**, 391 (2006), <https://doi.org/10.1364/JOSAB.23.000391>
16. J.B. Pendry, A.J. Holden, D.J. Robbins, W.J. Stewart, Magnetism from conductors and enhanced nonlinear phenomena, *IEEE Trans. Microw. Theory Tech.* **47**, 2075 (1999), <https://doi.org/10.1109/22.798002>
17. D.R. Smith, W.J. Padilla, D.C. Vier, S.C. Nemat-Nasser, S. Schultz, Composite medium with simultaneously negative permeability and permittivity, *Phys. Rev. Lett.* **84**, 4184 (2000), <https://doi.org/10.1103/PhysRevLett.84.4184>
18. B.A. Munk, *Frequency selective surfaces: theory and design* (Wiley, 2000)
19. F. Costa, A. Monorchio, A frequency selective radome with wideband absorbing properties, *IEEE Trans. Antennas Propag.* **60**, 2740 (2012), <https://doi.org/10.1109/TAP.2012.2194640>

20. J.F. Kang, Z. Qu, J.P. Duan, H.H. Jing, J.X. Hao, C.W. Song, J.Y. Wang, B.Z. Zhang, Multispectral flexible ultrawideband metamaterial absorbers for radar stealth and visible light transparency, *Opt. Mater.* **135**, 113351 (2023), <https://doi.org/10.1016/j.optmat.2022.113351>
21. Y. An, J. Qin, K. Sun, J. Tian, R. Fan, Carbon fiber skeleton/silver nanowires composites with tunable negative permittivity behavior, *EPJ Appl. Metamat.* **8**, 1 (2021), <https://doi.org/10.1051/epjam/2020010>
22. Z.H. Yang, Y.X. Che, X. Sun, J.L. Zhang, J.X. Tian, H.T. Yu, Q. Huang, Broadband polarization-insensitive microwave-absorbing composite material based on carbon nanotube film metamaterial and ferrite, *J. Appl. Phys.* **125**, 184902 (2019), <https://doi.org/10.1063/1.5086315>
23. L.J. Qu, C. Yang, S.J. Tan, Y. Xiao, Y. Wu, H.C. Chang, L. Xiao, G.B. Ji, A microwave absorption/infrared dual-band dynamic stealth regulator based on the carbon nanotube film and metamaterial, *Mater. Today Nano* **29**, 100556 (2025), <https://doi.org/10.1016/j.mtnano.2024.100556>
24. Z. Zhang, Y. Zhao, G. Fan, W. Zhang, Y. Liu, J. Liu, R. Fan, Paper-based flexible metamaterial for microwave applications, *EPJ Appl. Metamat.* **8**, 6 (2021), <https://doi.org/10.1051/epjam/2021003>
25. N.I. Landy, S. Sajuyigbe, J.J. Mock, D.R. Smith, W.J. Padilla, Perfect metamaterial absorber, *Phys. Rev. Lett.* **100**, 207402 (2008), <https://doi.org/10.1103/PhysRevLett.100.207402>
26. H. Tao, N.I. Landy, C.M. Bingham, X. Zhang, R.D. Averitt, W.J. Padilla, A metamaterial absorber for the terahertz regime: design, fabrication and characterization, *Opt. Express* **16**, 7181 (2008), <https://doi.org/arXiv:0803.1646>
27. A.E. Ruehli, G. Antonini, L. Jiang, *The partial element equivalent circuit method for electro-magnetic and circuit problems: a paradigm for EM modeling* (John Wiley & Sons, 2016)
28. D.R. Smith, D.C. Vier, T. Koschny, C.M. Soukoulis, Electromagnetic parameter retrieval from inhomogeneous metamaterials, *Phys. Rev. E* **71**, 036617 (2005), <https://doi.org/10.1103/PhysRevE.71.036617>
29. R. Liu, T.J. Cui, D. Huang, B. Zhao, D.R. Smith, Description and explanation of electromagnetic behaviors in artificial metamaterials based on effective medium theory, *Phys. Rev. E* **76**, 026606 (2007), <https://doi.org/10.1103/PhysRevE.76.026606>
30. D.R. Smith, Analytic expressions for the constitutive parameters of magnetoelectric metamaterials, *Phys. Rev. E* **81**, 036605 (2010), <https://doi.org/10.1103/PhysRevE.81.036605>
31. A.F. Koenderink, A. Alu, A. Polman, Nanophotonics: shrinking light-based technology, *Science* **348**, 516 (2015), <https://doi.org/10.1126/science.1261243>
32. M. Qu, T. Chang, G. Guo, S. Li, Design of graphene-based dual-polarized switchable rasorber/absorber at terahertz, *IEEE Access* **8**, 139482 (2020), <https://doi.org/10.1109/ACCESS.2020.3012745>
33. Z. Xue, S. Zhong, Y. Ma, Graphene-FSS hybrid absorptive structure with amplitude/frequency dual-modulated passband, *IEEE Antennas Wirel. Propag. Lett.* **20**, 1794 (2021), <https://doi.org/10.1109/LAWP.2021.3096196>
34. B.A. Chen, B. Wu, Y.T. Zhao, T. Su, Y.F. Fan, Via-based miniaturized rasorber using graphene films, *J. Appl. Phys.* **131**, 213102 (2022), <https://doi.org/10.1063/5.0091654>
35. B. Wu, D. Zhang, B. Chen, Y.J. Yang, Y.T. Zhao, T. Su, Broadband low-profile frequency selective rasorber using ultraminiaturized metal-graphene structure, *IEEE Antennas Wirel. Propag. Lett.* **21**, 2422 (2022), <https://doi.org/10.1109/LAWP.2022.3195811>
36. X. Pang, S. Mao, S. Sun, B. Wu, Lowpass frequency selective rasorber with wideband absorption using multilayer graphene-based metasurface, in *2022 International Conference on Microwave and Millimeter Wave Technology (ICMMT)*, 2022, pp. 1–3, <https://doi.org/10.1109/ICMMT55580.2022.10022672>
37. S.B. Mao, S.N. Sun, X.C. Liu, B. Wu, Graphene-based rasorber with wide transmission band and narrow transitional band, in *2021 IEEE MTT-S International Microwave Workshop Series on Advanced Materials and Processes for RF and THz Applications (IMWS-AMP)*, 2021
38. J. Yin, B. Wu, S.B. Mao, K.L. Wei, D. Zhang, X.Y. Pang, Y.T. Zhao, Broad-passband rasorber with ultrawideband absorption incorporating graphene-based resistive films and via-based winding inductors, *IEEE Antennas Wirel. Propag. Lett.* **23**, 4223 (2024), <https://doi.org/10.1109/LAWP.2024.3440319>
39. J.H. Yang, H.B. Zheng, Y.Q. Pang, B.Y. Qu, Y.F. Li, J.F. Wang, Z. Xu, Design, modelling, and manufacturing of sandwich radome structure with out-of-band absorption and in-band transmission performances, *Compos. Struct.* **339**, 118138 (2024), <https://doi.org/10.1016/j.compstruct.2024.118138>
40. J.H. Yang, Y.Q. Pang, G.D. Cai, J.F. Wang, Y.F. Li, H.B. Zheng, Z. Xu, Integrated design, modeling, and manufacturing of rasorber radome composites with electrically tunable transmission and wideband absorption properties, *Compos. Part B Eng.* **300**, 112467 (2025), <https://doi.org/10.1016/j.compositesb.2025.112467>
41. H. Chen, X.L. Peng, X.Z. Bo, M.Y. Geng, X.L. Yang, J.L. Zhan, Z.G. Liu, Y.Q. Dai, W.B. Lu, All-fabric flexible frequency-selective-rasorber based on cutting-transfer patterning method, *Adv. Mater. Interfaces* **9**, 2200651 (2022), <https://doi.org/10.1002/admi.202200651>
42. Y. Han, J.J. Chen, T. Fu, Q. Xue, W.Q. Che, Frequency selective absorbers based on aramid-paper honeycomb structures, *IEEE Trans. Electromagn. Compat.* **67**, 459 (2025), <https://doi.org/10.1109/TEM.2024.3477634>
43. K.W. Deng, F.P. Li, X.Y. Wang, J.Q. Feng, C. Xu, A compact frequency-selective absorber with optical transparency, *Mater. Res. Express* **11**, 025801 (2024), <https://doi.org/10.1088/2053-1591/ad2a86>
44. D. Yi, X.C. Wei, B. Shen, Y. Li, W. Zheng, X.K. Gao, Y.B. Yang, A rasorber-like waveguide based on thin film, *IEEE Microw. Wirel. Compon. Lett.* **28**, 558 (2018), <https://doi.org/10.1109/LMWC.2018.2838345>
45. M. Lin, J. Yi, X. Chen, Z.H. Jiang, L. Zhu, P. Qi, S.N. Burokur, Compact multi-functional frequency-selective absorber based on customizable impedance films, *Opt. Express* **29**, 14974 (2021), <https://doi.org/10.1364/OE.422071>
46. C.X. Fan, K. Duan, K. Chen, T. Jiang, J.M. Zhao, Y.J. Feng, Actively tunable rasorber with broadband RCS reduction and low infrared emissivity, *Opt. Express* **31**, 23294 (2023), <https://doi.org/10.1364/OE.494952>
47. X.K. Kong, W.H. Lin, X.M. Wang, L. Xing, S.L. Jiang, L.Q. Kong, M.L. Liu, Liquid reconfigurable stealth window constructed by a metamaterial absorber, *J. Opt. Soc. Am. B* **38**, 3277 (2021), <https://doi.org/10.1364/JOSAB.438914>

48. X. Ma, C.J. Guo, C. Huang, Y. Yuan, Y.N. Wang, X.J. Huang, J. Ding, X.Y. Pang, Flexible and transparent ultra-broadband low-profile frequency selective rasorber, *Opt. Express* **32**, 32435 (2024), <https://doi.org/10.1364/OE.532805>
49. Z.Y. Sun, J.L. Chen, S.M. Zhang, S.F. Tao, Design of low band transmission and high band absorption FSR based on coding metasurface, in *2024 IEEE 10th International Symposium on Microwave, Antenna, Propagation and EMC Technologies for Wireless Communications (MAPE)*, 2024, pp. 1–3, <https://doi.org/10.1109/MAPE62875>
50. Z.M. An, T.T. Xu, Y.P. Li, R.B. Zhang, B.Z. Zhang, Frequency selective rasorber with high temperature resistance and mechanical bearing characteristics based on double-layer metasurface regulation, *Mater. Des.* **254**, 113991 (2025), <https://doi.org/10.1016/j.matdes.2025.113991>
51. S.M. Zhang, Z.Y. Sun, T. Sun, J.Y. Zheng, S.F. Tao, Multi-objective optimization design of dual-polarized broadband frequency selective rasorber, *Microw. Opt. Technol. Lett.* **67**, 70383 (2025), <https://doi.org/10.1002/mop.70383>
52. S.X. Yu, N. Kou, Z. Ding, Z.P. Zhang, Harmonic-suppressed frequency selective rasorber using resistive-film sheet and square-loops resonator, *IEEE Antennas Wirel. Propag. Lett.* **19**, 292 (2020), <https://doi.org/10.1109/LAWP.2019.2960288>
53. J.M. Zhou, S.X. Yu, N. Kou, A frequency selective rasorber with absorption bands on both sides of passband based on screen-printed resistive film, *IEEE Antennas Wirel. Propag. Lett.* **23**, 3912 (2024), <https://doi.org/10.1109/LAWP.2024.3436912>
54. W.P. Wan, Y.F. Li, H. Wang, Z.B. Zhu, Y. Cheng, L.X. Jiang, L. Zheng, J.F. Wang, S.B. Qu, Chiral absorber-based frequency selective rasorber with identical filtering characteristics for distinct polarizations, *IEEE Trans. Antennas Propag.* **70**, 3506 (2022), <https://doi.org/10.1109/TAP.2021.3137467>
55. X.K. Kong, Z.W. Cao, X.M. Wang, W.H. Lin, Y.K. Zou, H. Wang, X.Y. Zhang, L.L. Wang, L. Xing, S. Gao, Wide-passband reconfigurable frequency selective rasorber design based on fluidity of EGaIn, *IEEE Antennas Wirel. Propag. Lett.* **22**, 1922 (2023), <https://doi.org/10.1109/LAWP.2023.3269506>
56. L.S. Wang, Q.H. Fu, F.S. Wen, X. Zhou, X.Y. Ding, Y. Wang, A thermally controlled multifunctional metamaterial absorber with switchable wideband absorption and transmission at THz band, *Materials* **16**, 846 (2023), <https://doi.org/10.3390/ma16020846>

Cite this article as: Jiahua Yang, Kun Zhang, Lan Yao, Resistive film frequency selective rasorbers: from design, integration to function, *EPJ Appl. Metamat.* **13**, 6 (2026). <https://doi.org/10.1051/epjam/2025014>